Journal of Power Sources 186 (2009) 22–28

Contents lists available at ScienceDirect

Journal of Power Sources

journal homepage: www.elsevier.com/locate/jpowsour

Proton-conducting membranes with high selectivity from cross-linked poly(vinyl alcohol) and poly(vinyl pyrrolidone) for direct methanol fuel cell applications

Y.F. Huang[a], L.C. Chuang[a], A.M. Kannan[b], C.W. Lin[a,*]

[a] Department of Chemical and Materials Engineering, National Yunlin University of Science and Technology, Yunlin 64002, Taiwan
[b] Electronic Systems Department, Arizona State University at the Polytechnic Campus, Mesa, AZ 85212, USA

ARTICLE INFO

Article history:
Received 13 June 2008
Received in revised form
18 September 2008
Accepted 19 September 2008
Available online 30 September 2008

Keywords:
Proton-conducting membrane
Semi-interpenetrating network
Poly(vinyl alcohol)
Membrane electrode assembly
Direct methanol fuel cells

ABSTRACT

A series of hydrocarbon membranes consisting of poly(vinyl alcohol) (PVA), sulfosuccinic acid (SSA) and poly(vinyl pyrrolidone) (PVP) were synthesized and characterized for direct methanol fuel cell (DMFC) applications. Fourier transform infrared (FT-IR) spectra confirm a semi-interpenetrating (SIPN) structure based on a cross-linked PVA/SSA network and penetrating PVP molecular chains. A SIPN membrane with 20% PVP (SIPN-20) exhibits a proton conductivity value comparable to Nafion® 115 (1.0×10^{-2} S cm^{-1} for SIPN-20 and 1.4×10^{-2} S cm^{-1} for Nafion® 115). Specifically, SIPN membranes reveal excellent methanol resistance for both sorption and transport properties. The methanol self-diffusion coefficient through a SIPN-20 membrane conducted by pulsed field-gradient nuclear magnetic resonance (PFG-NMR) technology measures 7.67×10^{-7} cm^2 s^{-1}, which is about one order of magnitude lower than that of Nafion® 115. The methanol permeability of SIPN-20 membrane is 5.57×10^{-8} cm^2 s^{-1}, which is about one and a half order of magnitude lower than Nafion® 115. The methanol transport behaviors of SIPN-20 and Nafion® 115 membranes correlate well with their sorption characteristics. Methanol uptake in a SIPN-20 membrane is only half that of Nafion® 115. An extended study shows that a membrane-electrode assembly (MEA) made of SIPN-20 membrane exhibits a power density comparable to Nafion® 115 with a significantly higher open current voltage. Accordingly, SIPN membranes with a suitable PVP content are considered good methanol barriers, and suitable for DMFC applications.

1. Introduction

Polymer electrolytes play an important role in fuel cell technology because they conduct protons from anode to cathode and prevent the fuel (hydrogen, methanol) from directly contacting oxygen. A perfluorosulfonic acid membrane called Nafion® (DuPont) is widely used as a proton conducting electrolyte membrane due to its excellent proton conductivity, good chemical resistance, and high mechanical properties. However, its relatively high price and high methanol crossover rate remain serious problems to its application in commercial direct methanol fuel cells (DMFCs) [1]. Its high methanol permeability not only reduces fuel efficiency, but also causes depolarization losses at the cathode [2,3]. Therefore, investigating new proton exchange membranes (PEMs) with low methanol permeability and suitable proton conductivity is crucial. However, high proton conductivity is usually accompanied by high methanol permeability, which makes it especially difficult to develop novel PEMs.

Water content has a profound effect on proton conductivity, methanol permeability, and the mechanical properties of proton exchange membranes. In general, high water uptake in membranes helps promote proton conduction because water is the primary proton carrier. However, the excessive water swelling is also an important factor for developing PEMs, which induces high methanol permeability and low mechanical strength in PEMs [4]. In addition, the excessive swelling also caused a tendency of delamination of MEAs during cell operation, making MEAs deteriorate due to the poor adhesion between membranes and gas diffusion electrodes [5]. Several previous attempts have been made to inhibit excessive PEM swelling [6–16]. These approaches included the use of chemical cross-linking structures [6–7], acid–base polymer blends [8–11], high molecular weight polymers [12–14], and membrane morphology control [15,16]. For all these approaches, the selection of a polymer matrix for the PEM is also an important factor because the swellability and methanol permeability of membranes is largely dependent upon polymer properties.

* Corresponding author. Tel.: +886 5 534 2601x4613; fax: +886 5 531 2071.
E-mail address: lincw@yuntech.edu.tw (C.W. Lin).

0378-7753/$ – see front matter © 2008 Elsevier B.V. All rights reserved.
doi:10.1016/j.jpowsour.2008.09.072

Poly(vinyl alcohol) (PVA) membranes are used in pervaporation-based alcohol dehydration because they preferentially permeate water and retain alcohol [17–20]. However, even though PVA membranes select water over alcohols, they are poor proton conductors. Therefore, several methods have been reported to prepare PVA-based proton conducting membranes with high proton conductivity for fuel cell applications [21–27]. Recently, Qiao et al. [28] used poly(vinyl pyrrolidone) (PVP) as a third polymer to modify PVA/poly(2-acrylamido-2-methyl-1-propanesulfonic acid) (PAMPS) polymer blends. They reported that the PVP polymer employed in the membranes can efficiently improve the oxidative stability and mechanical properties of the membranes. Another study reports the exceptional water or methanol sorption selectivity of poly(vinyl alcohol)/poly(vinyl pyrrolidone) blends [29].

However, an excessive swelling phenomenon usually exists in PVA/PVP-based membranes. For example, a water uptake of PVA/PAMPS/PVP membrane with proton conductivity comparable to Nafion® measured 100 wt.% was reported [28]. A high degree of swelling may cause failure in mechanical property to fabricate membrane electrode assemblies (MEAs) and a restriction to further reduction of methanol permeability in membrane. To our knowledge, no previous study investigated the methanol sorption and diffusion properties of PVA/PVP-based membranes as well as the performances of the single cells made use of such kind of membranes. Therefore, this study synthesizes a series of semi-interpenetrating network (SIPN) membranes using poly(vinyl alcohol) with sulfosuccinic acid (SSA) as a cross-linking agent and poly(vinyl pyrrolidone) as a modifier. A network based on PVA and SSA molecules not only inhibit the excessive swelling but also provides proton conducting paths. Moreover, the influence of penetrating poly(vinyl pyrrolidone) polymers is defined by membrane properties in terms of water uptake, self-diffusion coefficient, proton conductivity, and methanol permeability. In addition, an optimum SIPN membrane with 20% PVP was selected to fabricate membrane electrode assemblies to demonstrate the potential of SIPN membranes in DMFC applications. The DMFC performance of the SIPN-20 membrane exhibits a power density comparable to that of Nafion® 115, and the open current voltage of the SIPN-20 membrane is significantly higher than that of Nafion® 115. The SIPN membranes are therefore considered suitable for DMFC applications.

2. Experimental

2.1. Materials

Poly(vinyl alcohol) (PVA, average MW: 130,000 g mol^{-1}; degree of hydrolysis: 88%, Fluka), sulfosuccinic acid (SSA, 70 wt.% solution in water, Aldrich), poly(vinyl pyrrolidone) (PVP, average MW: 360,000 g mol^{-1}, Aldrich) were used to prepare proton conducting membranes. All chemicals were used without further purification. Pt/C (50% Pt on carbon black – Johnson Matthey, USA) was used as cathode electrocatalyst and Pt–Ru (58.1% Pt:Ru on Vulcan XC-72; 1:1 a/o Pt:Ru – ETek, USA) was used as anode electrocatalyst.

2.2. Membrane preparation

PVA powders were dissolved in de-ionized water with continuous stirring at 60 °C to form a 10 wt.% PVA aqueous solution. A given amount of SSA of a desired concentration was then added to this PVA solution and the mixture was stirred continuously until a homogeneous solution was obtained. A certain amount of PVP was then added to the PVA/SSA solution and stirred at 60 °C until a homogeneous solution was obtained. The membranes were cast by pouring the solution onto Petri dishes and evaporating water at 60 °C for 16 h. Membranes were peeled off the dishes and annealed at 120 °C for 1 h. The amount (%) of SSA and PVP were determined by the weight of PVA (i.e. a PVA/SSA50/PVP20 membrane was consisting of 1 g PVA, 0.5 g SSA, and 0.2 g PVP). After sudden cooling to room temperature, the resultant membranes were stored in deionized water.

2.3. Fourier transform infrared (FT-IR) spectroscopy

Infrared spectra were recorded in the transmittance mode on a Fourier transform infrared spectrophotometer (FT-IR, PerkinElmer, Spectrum One) in the range of wavenumbers 600–4000 cm^{-1}. The resolution and number of scans in all spectra were 4 cm^{-1} and 16, respectively.

2.4. Water uptake, ion-exchange capacity (IEC), and water states in membrane

The water uptake of the membrane was determined by measuring the change in weight before and after hydration. The membrane was immersed in deionized water for 24 h. The wetted membrane weight (W_{wet}) was then measured as soon as the surface-attached water on the membrane was removed with filter paper. The weight of the dry membrane (W_{dry}) was determined after drying it in a vacuum at 60 °C for 1 day. The water uptake (%) was calculated using the following equation:

$$\text{Water uptake}\,(\%) = \frac{W_{wet} - W_{dry}}{W_{dry}} \times 100$$

Ion-exchange capacities (IEC) of the samples were estimated by a titration method. The ion-exchange capacity was calculated using the following equation:

$$\text{IEC} = \frac{M_{i,\,NaOH} * M_{f,\,NaOH}}{W_{dry}} = \frac{H^{+}(\text{mmol})}{W_{dry}}$$

where $M_{i,NaOH}$ is the initial mmol of NaOH of titration and $M_{f,NaOH}$ is the mmol (m_{eq}) of NaOH after equilibrium. H^+ is the molar number of proton sites presented in the membrane, and W_{dry} is the weight (g) of the dry membrane.

Two types of water, freezing water (unbound water) and non-freezing water (bound water) in fully hydrated membranes were determined using a differential scanning calorimeter (DSC 2010, TA Instruments) equipped with a rapid cooling system (RCS). The experiment began with heating the sample from −50 to 50 °C using a heating rate of 3 °C min^{-1} and a nitrogen gas flow rate of 50 mL min^{-1}. The freezing water content was determined using following equation:

$$m_{free} = \frac{\Delta H_{free}}{Q_{melting}} \times m_{total}$$

where $Q_{melting}$ is the melting enthalpy of pristine water at 0 °C, ΔH_{free} is the heat of melting around 0 °C, and m_{total} is the total uptake water.

2.5. Water and methanol self-diffusion coefficients

Self-diffusion coefficients were measured with a Varian UNITY INOVA-500 MHz Nuclear Magnetic Resonance (NMR) spectrometer at an applied gradient strength ranging from 0 to 200 G cm^{-1}. Experiments were conducted at room temperature and a total of ten

points were recorded with decreasing gradient strengths. Before testing, the membranes were soaked in water and methanol for at least 1 day. After removing any surface solvent, the membranes were quickly placed in a NMR tube and sealed. The signal intensity (A) as a function of the gradient strength (G) was recorded. Stejskal and Tanner [30] reported that the predicted dependence of signal attenuation on gradient strength is

$$\ln \frac{A(2\tau)}{A_0(2\tau)} = -\left[(\gamma_H G\delta)^2 \left\langle \Delta - \frac{\delta}{3} \right\rangle\right] D$$

where $A(g)$ is the signal intensity as a function of the applied gradient g, $A(0)$ is the signal intensity observed in the absence of an applied gradient, γ is the nuclear gyromagnetic ratio, D is the water diffusion coefficient, δ is the length of the gradient pulse, and Δ is the diffusion time between gradient pulses.

2.6. Proton conductivity and methanol permeability

Proton conductivity measurements were carried out at ambient temperature using an Autolab PGSTAT30 instrument. Before test, the membrane was immersed in deionized water for 1 day. The proton conductivity cell was composed of two 9.5 mm diameter stainless steel electrodes. The membrane sample was sandwiched between the stainless steel electrodes. The AC impedance spectra of the membranes were recorded from 200,000 to 100 Hz with amplitude of 5 mV. The proton conductivity was calculated according to

$$\sigma = \frac{L}{R \cdot A}$$

where σ, L, R, and A denote the proton conductivity of membrane, thickness of the membrane (which was measured with a micrometer in each case), the measured resistance of the membrane, and the cross-sectional area of the membrane perpendicular to current flow, respectively.

The methanol permeability of membrane was determined using a home-made side-by-side glass diffusion cell containing 3 wt.% methanol solution in one side and pure water in the other side. The diffusion cell was maintained at a temperature of 35 °C. The different methanol concentrations between the two compartments caused a flux of methanol across the membrane. Methanol concentration within the water side was measured using gas chromatography (GC, China Chromatography 9800) at regular intervals. Methanol permeability was determined from the slope of the plot of methanol concentration in the receptor compartment versus time.

2.7. Fabrication of membrane electrode assembly (MEA) and evaluation of single cell performance

The SIPN membrane-based MEA was fabricated using CARBEL CL gas diffusion media (W. L. Gore and Associates, Inc., Elkton, MD) as a support. The cathode was created by layering carbon supported Pt bound with Nafion® electrolyte as a catalyst layer on this diffusion layer to give a metal loading of 3 mg cm^{-2}. The anode was constructed using the same method, except that carbon supported Pt–Ru served as anode catalyst for the DMFC. Methanol flow rate was fixed at 3 cc min^{-1} and oxygen flow rate was fixed at 100 SCCM. For comparison, experiments were also carried out with the MEA fabricated with Nafion® 115 membrane under similar experimental conditions. The details of the MEA fabrication procedures and conditions were according to our previous work [31]. Single cell performance was evaluated using a MACCOR Model 2200 fuel cell test station.

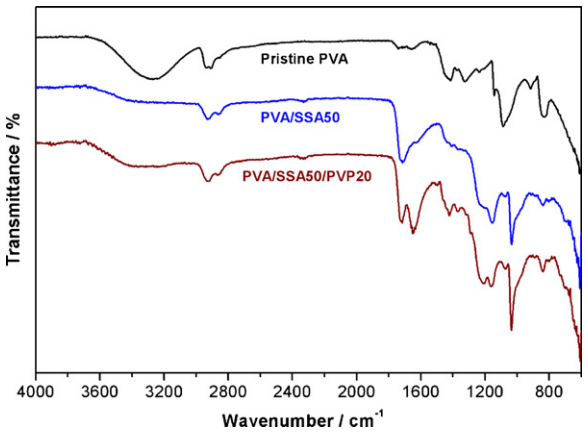

Fig. 1. FT-IR Spectra of PVA, PVA/SSA and PVA/SSA/PVP membranes.

3. Results and discussion

3.1. FT-IR study

Fig. 1 shows the FT-IR spectra for pristine PVA, PVA/SSA, and PVA/SSA/PVP membranes. The PVA/SSA membrane shows characteristic absorption bands at 1716 cm^{-1}(C=O) and the ester group C–O stretch mode at 1208 cm^{-1}. Ester group formation is caused by ester bonds (C–O–C) between the PVA alcohol groups and SSA carboxyl groups. Furthermore, the absorption band observed at 1034 cm^{-1} is attributed to –SO_3 groups in the SSA. For the PVA/SSA/PVP membrane, the stretching vibration of hydrogen bonded carbonyl groups (C=O) on PVP was also observed at 1651 cm^{-1} [32]. This absorption band confirms the intermolecular interactions between the hydroxyl groups on PVA and carbonyl groups on penetrating PVP in membranes. Fig. 2 illustrates the scheme of the SIPN structure. A SSA bridge between PVA molecules not only reinforces the network, but also provides a primary proton conducting path. However, a membrane with a high degree of cross-linkage through ester bond formation between PVA and SSA often has a brittle nature and serious hydrolysis problems. PVP chains trapped in the network form a semi-interpenetrating network (SIPN) structure, which presumably stabilizes the network structure through hydrogen bonds and reduces the brittleness of the membranes.

3.2. Water uptake and ion-exchange capacity

Fig. 3 shows that water uptake in the SIPN membrane (based on 40% PVP) depends on the SSA content in that water uptake

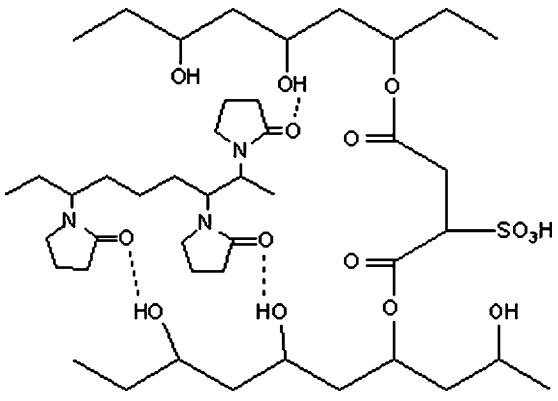

Fig. 2. The SIPN structural scheme of the PVA/SSA/PVP membrane.

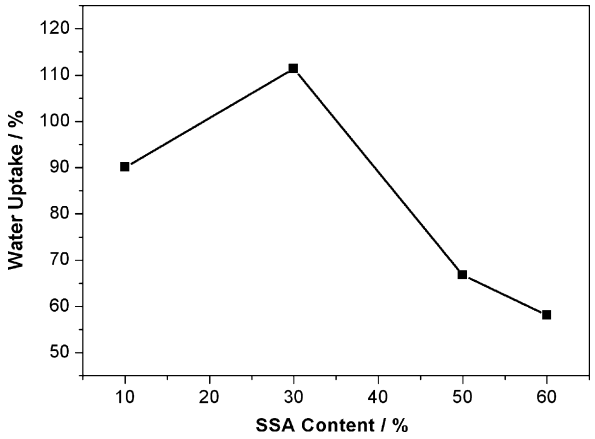

Fig. 3. Water uptakes of PVA/PVP40 membrane with different amounts of SSA.

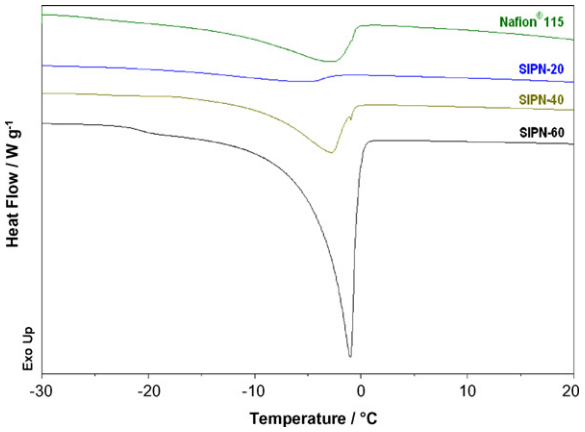

Fig. 5. DSC curves of Nafion® 115 and SIPN membranes based on PVA/SSA50 with different amounts of PVP.

increases as the SSA content increases from 10% to 30%, and then decreases when the SSA content exceeds 30%. Inverse behaviors can be explained by the chemical structure of the PVA/SSA network. An increase in water uptake at a low SSA content may be the result of an increase in the sulfonic acid group in the PVA/SSA/PVP membranes. However, higher cross-linking density in the SIPN membranes at a higher SSA content may create a more rigid and compact polymer structure. In addition, when the SSA content exceeds 60%, the membranes become too brittle for fuel cell applications. Accordingly, to fulfill the SIPN membrane requirements of suitable water uptake and mechanical properties, all the samples reported in this study are based on 50% SSA (i.e. PVA/SSA50) interpenetrated with various amounts of PVP to help stabilize the network and determine the effect of PVP interpenetration on the corresponding properties of SIPN membranes.

Fig. 4 shows the measured IEC and water uptake of the SIPN membranes as a function of PVP content. As Fig. 4 shows, the measured IEC value of the SIPN membranes decreases as the PVP content increases from 10% to 60%. On the other hand, the water uptake of SIPN membranes increases from 43.7% to 127.9% as the PVP content increases. The lack of the cation exchange groups and the hydrophilic property of PVP, respectively, explain these results.

3.3. Water states

This study groups water in polymers by different states as free water, freezable bound water, and non-freezing water. Respectively, these terms refer to water that is strongly bound to sulfonic acid groups (non-freezing water), weakly bound to polymer chains (freezable bound water), and water that has the same properties as bulk water (free water) [33]. Liu et al. [34] reported the bound water has a markedly reduced mobility compared to free water. This result indicates that membranes with different water state distributions may exhibit different transport properties. Therefore, this study uses a DSC to determine the distributions of bound and unbound water existing in the membranes.

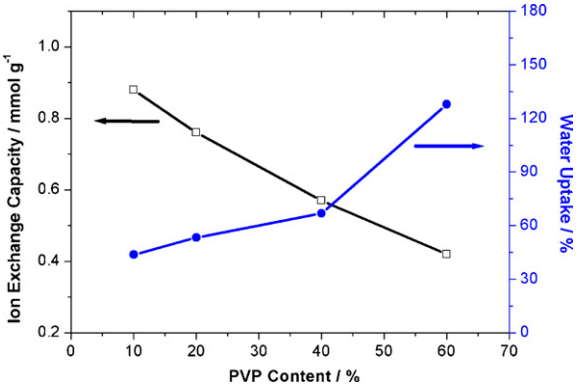

Fig. 4. IEC and water uptakes of SIPN membranes based on PVA/SSA50 with different amounts of PVP.

Fig. 5 shows the DSC curves of fully hydrated SIPN and Nafion® 115 membranes. Melting enthalpy peaks appear at temperatures around 0 °C, and the peak area increases as the PVP content increases from 20% to 60%. Table 1 summarizes the distribution of water states in SIPN and Nafion® 115 membranes in terms of bound and unbound water. As Table 1 shows, the SIPN membrane holds more unbound water as the PVP content increases. This is primarily due to an increase of hydrophilic groups in the membranes.

3.4. Proton conductivity

Fig. 6 presents the proton conductivity of the SIPN membranes as a function of PVP content at room temperature. The proton conductivity of Nafion® 115 measured under the same experimental conditions was 1.4×10^{-2} S cm^{-1}, which agrees well with the literature [35,36]. As Fig. 6 shows, the proton conductivity of SIPN membranes increases as the PVP content increases from 10% to 20%, reaching a maximum value of 0.01 S cm^{-1} when PVP content reaches 20%. These membranes then experience a decrease in proton conductivity when the PVP content exceeds 20%. The inverse behaviors of the water uptake and the ion-exchange capacity (IEC) explain this behavior, as Fig. 4 shows. These results indicate that an increase in water content can lead to higher proton conductivity at a low PVP content. However, large sorption of water in membranes does not simply improve proton conductivity, but also dilutes the charge carries [28], which causes a decrease in proton conductivity at high PVP contents in SIPN membranes.

3.5. Water/methanol uptake

This study investigates the sorption and transport properties of water and methanol in SIPN-20 membranes and compares these properties with Nafion® 115 to further investigate the potential of SIPN membranes for DMFC applications. Fig. 7 shows the solvent uptake of Nafion® 115 and PVA/SSA50/PVP20 (SIPN-20) membranes as a function of methanol concentration. The solvent uptake

Table 1
The distribution of water state in various SIPN and Nafion® 115 membranes.

Membrane	Water uptake (wt.%)	ΔH_{free} (J g^{-1})	Unbound water (wt.%)	Bound water (wt.%)	Water state distribution (%)	
					Unbound water/total water	Bound water/total water
SIPN-20	53.29 ± 7.0	5.89	1.76	51.53	3.31	96.69
SIPN-40	66.76 ± 7.7	20.67	6.19	60.57	9.27	90.73
SIPN-60	127.91 ± 15.2	65.64	19.65	108.26	15.36	84.64
Nafion® 115	37.0 ± 3.3	28.2	8.44	28.56	22.82	77.18

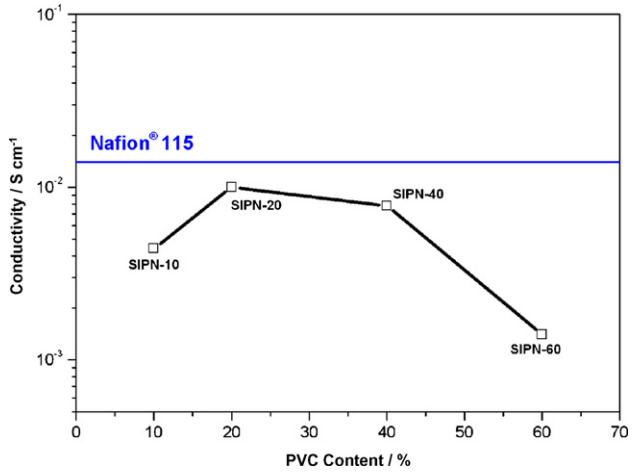

Fig. 6. Proton conductivities of SIPN membranes based on PVA/SSA50 with different amounts of PVP.

of Nafion® 115 increases through a maximum value at a methanol mole fraction 0.63. This trend agrees well with the literature [37]. On the other hand, the SIPN-20 membrane exhibits a higher water uptake than Nafion® 115 and then takes up less solvent as the methanol mole fraction increases. Specifically, the methanol uptake of a SIPN-20 membrane is approximately one half that of Nafion® 115.

These different sorption behaviors can be explained by the chemical cross-linking structure of SIPN membranes versus the physical cross-linking structure of Nafion® 115. The excellent methanol-resistant nature of PVA is also an important factor [38]. A similar finding by Lu et al. [29] shows that PVA/PVP interpenetrating polymer network (IPN) membranes achieve an exceptional selectivity in sorption of water over methanol in terms of swelling ratio.

Table 2
The water and methanol self-diffusion coefficients of various SIPN and Nafion® 115 membranes.

Membrane	D_{H_2O} (cm^2 s^{-1})	D_{CH_3OH} (cm^2 s^{-1})	D_{CH_3OH}/D_{H_2O}
Water [a]	2.3×10^{-5}	N/A	N/A
Methanol[a]	N/A	2.4×10^{-5}	N/A
SIPN-20	$1.35 \times 10^{-6} \pm 2.7 \times 10^{-8}$	$7.67 \times 10^{-7} \pm 1.4 \times 10^{-8}$	0.568
SIPN-40	$8.11 \times 10^{-6} \pm 3.6 \times 10^{-7}$	$8.64 \times 10^{-7} \pm 3.6 \times 10^{-8}$	0.107
SIPN-60	$1.11 \times 10^{-5} \pm 1.4 \times 10^{-7}$	$5.83 \times 10^{-6} \pm 1.1 \times 10^{-7}$	0.525
Nafion[a]	8.0×10^{-6}	9.0×10^{-6}	1.125

[a] Data obtained from Ref. [39].

3.6. Water and methanol self-diffusion coefficients

Table 2 shows the water and methanol self-diffusion coefficients within SIPN and Nafion® 115 membranes. Both water and methanol self-diffusion coefficients within SIPN membranes increase when PVP content increases from 20% to 60%. This result correlates well to the increase of water uptake and unbound water in SIPN membranes. On the other hand, the water self-diffusion coefficient within the SIPN-20 membrane measures 1.35×10^{-6} cm^2 s^{-1}, about one-fifth that of Nafion® 115. The lower unbound water content in SIPN-20 membranes explains this performance. Liu and Yao [34] report that bound water has a markedly reduced mobility compared to free water. Specifically, note the methanol self-diffusion coefficient within the SIPN-20 membrane measures 7.67×10^{-7} cm^2 s^{-1}, about an order of magnitude lower than Nafion® 115. This lower methanol self-diffusion coefficient of SIPN-20 membrane can be attributed to its lower methanol uptake.

Table 2 compares the self-diffusion coefficient ratios of methanol to water, D_{CH_3OH}/D_{H_2O}. For Nafion®, the water and methanol self-diffusion coefficients exhibit no obvious differences [39]. On the other hand, Ren et al. [40] report that the solvent uptake per sulfonic acid group in Nafion® is the same for membranes equilibrated in pure water or pure methanol. These results indicate that Nafion® has no preference in either sorption or trans-

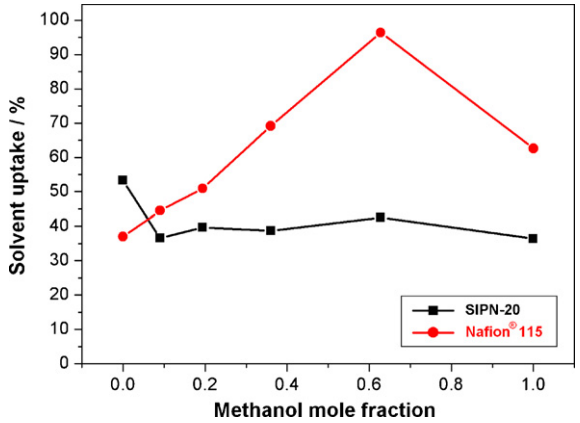

Fig. 7. Solvent uptake of Nafion® 115 and SIPN-20 membranes plotted against methanol concentration.

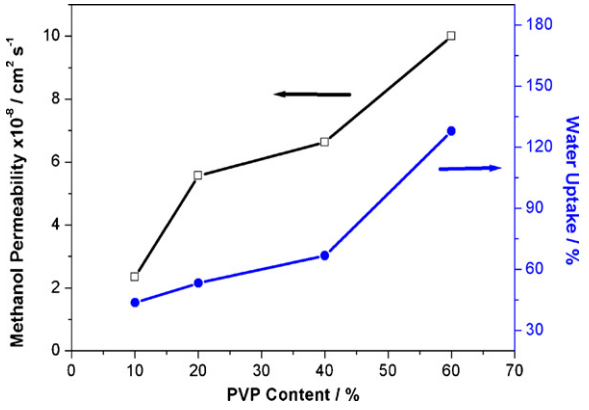

Fig. 8. Water uptakes and methanol permeabilities of SIPN membranes based on PVA/SSA50 with different amounts of PVP.

Table 3
The measured water uptake, proton conductivity, methanol permeability and selectivity of various SIPN and Nafion® 115 membranes.

Membrane	Water uptake (wt.%)	Conductivity (S cm^{-1})	Methanol permeability (cm^2 s^{-1})	Selectivity, φ ($\times 10^3$ S cm^{-3} s)
SIPN-10	43.71 ± 2.3	$4.4 \times 10^{-3} \pm 3 \times 10^{-4}$	$2.35 \times 10^{-8} \pm 1.2 \times 10^{-8}$	187
SIPN-20	53.29 ± 7.0	$1.0 \times 10^{-2} \pm 3 \times 10^{-3}$	$5.57 \times 10^{-8} \pm 3.5 \times 10^{-8}$	180
SIPN-40	66.76 ± 7.7	$7.8 \times 10^{-3} \pm 2 \times 10^{-4}$	$6.63 \times 10^{-8} \pm 4.1 \times 10^{-8}$	118
SIPN-60	127.91 ± 15.2	$1.4 \times 10^{-3} \pm 1 \times 10^{-4}$	$1.00 \times 10^{-7} \pm 5.5 \times 10^{-8}$	14
Nafion® 115	37.0 ± 3.3	$1.4 \times 10^{-2} \pm 2.5 \times 10^{-3}$	$1.8 \times 10^{-6} \pm 4 \times 10^{-8}$	7.8

port of water and methanol. Note that D_{CH_3OH}/D_{H_2O} in the SIPN-20 membrane is approximately half that of Nafion® (0.568 for SIPN-20 and 1.125 for Nafion®), suggesting that the SIPN-20 membrane has a higher selectivity in transport of water over methanol. This diffusion behavior is strongly correlated to the sorption behaviors of SIPN-20 and Nafion® membranes (Fig. 7). Accordingly, the SIPN-20 membrane clearly demonstrates higher selectivity in sorption and transport of water over methanol.

3.7. Methanol permeability and selectivity

Fig. 8 presents the methanol permeability of SIPN membranes as a function of PVP content. Methanol permeability in Nafion® 115 was measured under similar experimental conditions reported as 1.8×10^{-6} cm^2 s^{-1}. This value agrees well with the literature [41]. The methanol permeability of SIPN membranes increases from 2.35×10^{-8} to 1.00×10^{-7} cm^2 s^{-1} as PVP content increases, varying from 10% to 60%. Similar trends in the water uptake and methanol self-diffusion coefficient can be well correlated. Specifically, as Table 3 shows, all of the SIPN membranes show lower methanol permeability than Nafion® 115. For the SIPN-20 membrane, methanol permeability measures 5.57×10^{-8} cm^2 s^{-1}, which is about one and a half order of magnitude lower than that of Nafion® 115. The lower methanol permeability of the SIPN-20 membrane correlates to its lower methanol uptake and methanol self-diffusion coefficients. Note that the methanol permeability of the SIPN membranes based on PVA/SSA50/PVP is about one order of magnitude lower than the PVA/PAMPS/PVP membrane reported in the literature [28].

To explore the possibility of using SIPN membranes in DMFC applications, the selectivity of proton conductivity and methanol permeability should be analyzed. Notice that all of the SIPN membranes exhibit higher selectivity than Nafion® 115, as Table 3 shows. According to this result, SIPN membranes are suitable for use in DMFCs. Table 3 summarizes all the measured properties related to proton exchange membranes. It can be concluded that PVP plays a major role in controlling proton conduction and methanol permeability due to its hydrophilic groups.

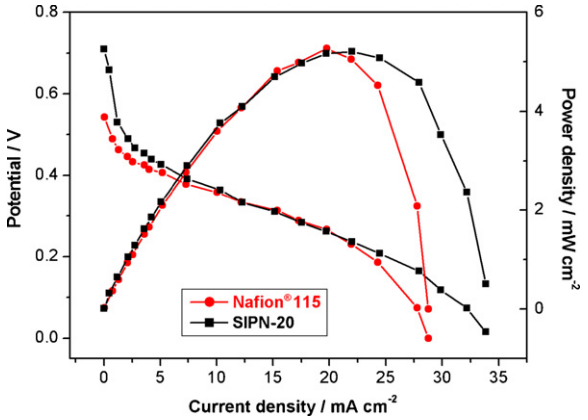

Fig. 9. DMFC performances of MEAs using SIPN-20 (PVA/SSA50/PVP20) and Nafion® 115 membranes at room temperature with 2 M methanol and oxygen at ambient pressure.

3.8. Single cell performance

Since the SIPN-20 membrane exhibits relatively high proton conductivity and good methanol resistance compared to other SIPN membranes, this study explores the DMFC performance of a SIPN-20 membrane-based membrane electrode assembly. Fig. 9 compares fuel cell performances of MEAs using SIPN-20 and Nafion® 115 membranes with 2 M methanol/O_2 at room temperature. The thicknesses of the SIPN-20 membrane were controlled in a range of 100–120 μm. As Fig. 9 shows, the SIPN-20 membrane-based MEA exhibits significantly higher open current voltage (OCV) than Nafion® 115, exceeding it by as much as 150 mV. This difference is mainly due to the very low methanol permeability of the SIPN-20 membrane. Importantly, both SIPN and Nafion115 membranes exhibit very close maximum power density, i.e. 5.20 mW cm^{-2} for SIPN-20 and 5.26 mW cm^{-2} for Nafion-115, respectively. These results clearly demonstrate the potential of SIPN membranes for DMFC applications.

4. Conclusion

This study reports the preparation of a series of SIPN proton conducting membranes using a cross-linked PVA/SSA network and penetrating PVP polymers. FT-IR spectra confirm the completion of cross-linking PVA/SSA reactions and intermolecular interactions between PVP and PVA. PVP has significant effects on the sorption and transport behavior of water in SIPN membranes. Due to the hydrophilic character of PVP, the water uptake, unbound water content, and water self-diffusion coefficients of SIPN membranes increase as the PVP content increases. The SIPN-20 membrane exhibits comparable proton conductivity to commercial Nafion® 115 with reasonable uptake water. Specifically, the methanol transport properties of the SIPN-20 membrane in terms of methanol self-diffusion coefficient and methanol permeability are significantly lower than those of Nafion® 115. The methanol permeability of the SIPN-20 membrane measures 5.57×10^{-8} cm^2 s^{-1}, which is about one and a half order of magnitude lower than Nafion® 115. The DMFC performance of a SIPN-20 membrane-based membrane-electrode assembly exhibits a power density comparable to Nafion® 115 but with a significantly higher open current voltage. These results indicate SIPN membranes with excellent methanol resistance are potential candidates as polymer electrolytes for DMFC applications.

Acknowledgements

The authors are grateful to the Energy Commission, Ministry of Economic Affairs and the National Science Council of Taiwan (ROC) for the financial support of this work through Grants 96-ET-7-224-001-ET and NSC96-2120-M-011-002, respectively. The assistance of PFG-NMR operation from the National Sun Yat-Sen University is also grateful.

References

[1] M. Doyle, G. Rajendran, in: W. Vielstich, H.A. Gasteiger, A. Lamm (Eds.), Handbook of Fuel Cells—Fundamentals, Technology and Applications, vol. 3, John Wiley and Sons, Chichester, 2003, pp. 351–395.
[2] X. Ren, P. Zelencsy, S. Thomas, J. Davey, S. Gottesfeld, J. Power Sources 86 (2000) 111.
[3] K. Lee, J.D. Nam, J. Power Sources 157 (2006) 201.
[4] H. Strathmann, Ion-Exchange Membrane Separation Processes, Membrane Science and Technology Series 9, Chapter 3, Elsevier Science Publisher, Amsterdam, 2004, pp. 118–121.
[5] J. Won, H.H. Park, Y.J. Kim, S.W. Choi, H.Y. Ha, I.H. Oh, H.S. Kim, Y.S. Kang, K.J. Ihn, Macromolecules 36 (2003) 3228.
[6] E.B. Easton, T.D. Astill, S. Holdcroft, J. Electrochem. Soc. 152 (2005) A752–A758.
[7] S.D. Mikhailenko, K. Wang, S. Kaliaguine, P. Xing, G.P. Robertson, M.D. Guiver, J. Membr. Sci. 233 (2004) 93.
[8] J. Kerres, A. Ullrich, F. Meier, T. Häring, Solid State Ionics 125 (1999) 243.
[9] M. Walker, K.M. Baumgärtner, M. Kaiser, J. Kerres, A. Ullrich, E. Räuchle, J. Appl. Polym. Sci. 74 (1999) 67.
[10] J. Kerres, J. Membr. Sci. 185 (2001) 3.
[11] H.L. Wu, C.C.M. Ma, C.H. Li, T.M. Lee, C.Y. Chen, C.L. Chiang, C. Wu, J. Membr. Sci. 280 (2006) 501.
[12] Y. Li, F. Wang, J. Yang, D. Liu, A. Roy, S. Case, J. Lesko, J.E. McGrath, Polymer 47 (2006) 4210.
[13] J. Qiao, H. Ono, T. Oishi, T. Okada, ECS Trans. 3 (2006) 97.
[14] H.L. Wu, C.C.M. Ma, H.C. Kuan, C.H. Wang, C.Y. Chen, C.L. Chiang, J. Polym. Sci. Polym. Phys. Ed. 44 (2006) 565.
[15] S. Swier, V. Ramani, J.M. Fenton, H.R. Kunz, M.T. Shaw, R.A. Weiss, J. Membr. Sci. 256 (2005) 122.
[16] S. Swier, M.T. Shaw, R.A. Weiss, J. Membr. Sci. 270 (2006) 22.
[17] J.W. Rhim, C.K. Yeom, S.W. Kim, J. Appl. Polym. Sci. 68 (1998) 1717.
[18] W.Y. Chiang, C.L. Chen, Polymer 39 (1998) 2227.
[19] J.W. Rhim, Y.K. Kim, J. Appl. Polym. Sci. 75 (2000) 1699.
[20] J.W. Rhim, M.Y. Sohn, H.J. Joo, K.H. Lee, J. Appl. Polym. Sci. 50 (1993) 679.
[21] B. Smitha, S. Sridhar, A.A. Khan, J. Appl. Polym. Sci. 95 (2005) 1154.
[22] M.S. Kang, J.H. Kim, J. Won, S.H. Moon, Y.S. Kang, J. Membr. Sci. 247 (2005) 127.
[23] D.S. Kim, M.D. Guiver, S.Y. Nam, T.I. Yun, M.Y. Seo, S.J. Kim, H.S. Hwang, J.W. Rhim, J. Membr. Sci 281 (2006) 156.
[24] J. Qiao, T. Hamaya, T. Okada, Chem. Mater. 17 (2005) 2413.
[25] C.S. Wu, F.Y. Lin, C.Y. Chen, P.P. Chu, J. Power Sources 160 (2006) 1204.
[26] J.W. Rhim, H.B. Park, C.S. Lee, J.H. Jun, D.S. Kim, Y.M. Lee, J. Membr. Sci. 238 (2004) 143.
[27] D.S. Kim, H.B. Park, J.W. Rhim, Y.M. Lee, J. Membr. Sci. 240 (2004) 37.
[28] J. Qiao, T. Hamaya, T. Okada, Polymer 46 (2005) 10809.
[29] J. Lu, Q. Nguyen, J. Zhou, Z.H. Ping, J. Appl. Polym. Sci. 89 (2003) 2808.
[30] E.O. Stejskal, J.E. Tanner, J. Chem. Phys. 42 (1965) 288.
[31] C.W. Lin, R. Thangamuthu, C.J. Yang, J. Membr. Sci. 253 (2005) 23.
[32] K. Lewandowska, Eur. Polym. J. 41 (2005) 55.
[33] K. Nakamura, T. Hatakeyama, H. Hatakeyama, Polymer 24 (1983) 871.
[34] W.G. Liu, K.D. Yao, Polymer 42 (2001) 3943.
[35] N.W. DeLuca, Y.A. Elabd, J. Membr. Sci. 282 (2006) 217.
[36] D.S. Kim, M.D. Guiver, S.Y. Nam, T.I. Yun, M.Y. Seo, S.J. Kim, H.S. Hwang, J.W. Rhim, J. Membr. Sci. 281 (2006) 156.
[37] E. Skou, P. Kauranen, J. Hentschel, Solid State Ionics 97 (1997) 333.
[38] B.S. Pivovar, Y. Wang, E.L. Cussler, J. Membr. Sci. 154 (1999) 155.
[39] S. Hietala, S.L. Maunu, F. Sundholm, J. Polym. Sci. Polym. Phys. Ed. 38 (2000) 3277.
[40] X. Ren, T.E. Springer, S. Gottesfeld, J. Electrochem. Soc. 147 (2000) 92.
[41] L. Li, J. Zhang, Y. Wang, J. Membr. Sci. 226 (2003) 159.